

AD737621

ROCK DISINTEGRATION BY PULSED LIQUID JETS

William C. Cooley
Paul E. Brockert

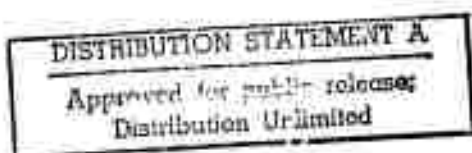
TERRASPACE INCORPORATED
Suite 320
5400 Pooks Hill Road
Bethesda, Maryland 20014

ANNUAL REPORT

Reproduced by
NATIONAL TECHNICAL
INFORMATION SERVICE
Springfield, Va. 22151

SPONSORED BY
Advanced Research Projects Agency
ARPA Order No. 1579, Amend. 2
Program Code 1F10

MONITORED BY
Bureau of Mines
Contract No. H0210012



44

The views and conclusions contained in this document are those of the authors and should not be interpreted as necessarily representing the official policies either expressed or implied, of the Advanced Research Projects Agency or the United States Government.

ACCESSION FOR	
CPSTI	WHITE SECTION <input checked="" type="checkbox"/>
DDC	BUFF SECTION <input type="checkbox"/>
UNANNOUNCED	<input type="checkbox"/>
JUSTIFICATION	
BY	
DISTRIBUTION/AVAILABILITY CODES:	
DIST.	AVAIL. and/or SPECIAL
A	

Unclassified

Security Classification

DOCUMENT CONTROL DATA - R & D

(Security classification of title, body of abstract and indexing annotation must be entered when the overall report is classified)

1. ORIGINATING ACTIVITY (Corporate author)

Terraspace, Incorporated
5400 Pooks Hill Road
Bethesda, Md. 20014

2a. HISTORY SECURITY CLASSIFICATION

Unclassified

2b. GROUP

3. REPORT TITLE

Rock Disintegration By Pulsed Liquid Jets

4. DESCRIPTIVE NOTES (Type of report and inclusive dates)

Annual Report, January 1971 through January 1972

5. AUTHOR(S) (First name, middle initial, last name)

William C. Cooley
Paul E. Brockert

6. REPORT DATE

January 1972

7a. TOTAL NO. OF PAGES

35

7b. NO. OF REFS

7

8a. CONTRACT OR GRANT NO.

HO-10012

8b. ORIGINATOR'S REPORT NUMBER(S)

TR-4032

b. PROJECT NO.

ARPA Order No. 1579

c.

Amendment 2

d.

Program Code 1F10

8b. OTHER REPORT NO(S) (Any other numbers that may be assigned this report)

10. DISTRIBUTION STATEMENT

Distribution of this document is unlimited

11. SUPPLEMENTARY NOTES

12. SPONSORING MILITARY ACTIVITY

Advanced Research Projects
Agency
Washington, D.C. 20301

13. ABSTRACT

Experiments are reported on the breakage of granite, limestone and sandstone by pulsed water jets using a Voitsekhovskiy-type cumulation nozzle with jet velocities up to 1800 m/sec, a jet diameter of 0.716 cm, and piston impact energies up to 65,000 Joules. Data on the specific energy for single pulse spall craters in the face of 30 cm cubic rock samples is plotted against the specific pressure (the ratio of jet stagnation pressure to rock compressive strength). The specific energy decreases rapidly as the jet stagnation pressure is increased, from 1.43 to 3.95 times the compressive strength. A specific energy of 500 J/cm³ was observed for Barre granite. The relatively low values of specific energy are attributed to the high jet pressure in combination with a relatively short length-to-diameter ratio of the water slug which produces shear fractures. Many of the test shots produced extensive tensile splitting or complete shattering of the 30 cm cubic samples. Therefore larger samples or in situ testing are required to evaluate the effectiveness of this type of nozzle for rock tunneling. No mechanical damage to the nozzle was observed after a total of 43 test shots.

14.

KEY WORDS

LINK A

LINK B

LINK C

ROLE

WT

ROLE

WT

ROLE

WT

Disintegration, Rock

Jet, Liquid

Nozzle, Exponential

Gun, Gas

**ROCK DISINTEGRATION BY PULSED LIQUID JETS
ANNUAL REPORT
JANUARY 1972
REPORT NO. TR-4032**

**Prepared By
Terraspace Incorporated
Suite 320
5400 Pooks Hill Road
Bethesda, Maryland 20014**

**William C. Cooley
Principal Investigator
Phone (301) 530-6035**

**Paul E. Brockert
Project Engineer
Phone (301) 424-0090**

**Sponsored By
Advanced Research Projects Agency
ARPA Order No. 1579, Amend. 2
Program Code 1F10**

**Monitored By
Bureau of Mines
Contract No. H0210012
Amount of Contract \$64,711.00
Effective Date: January 1, 1971
Contract Expiration: January 31, 1972**

TABLE OF CONTENTS

<u>Chapter</u>	<u>Page</u>
1.0 OBJECTIVES AND SCOPE	1
2.0 INTRODUCTION	2
3.0 EXPERIMENTAL EQUIPMENT	3
4.0 INSTRUMENTATION AND CONTROL	10
4.1 Piston Velocity Measurement	10
4.2 Chamber Pressure Measurement	10
4.3 Jet Velocity Measurement	10
5.0 TEST PROCEDURES	12
5.1 Tests with 3.0 kg Piston Impacting Water Package	12
5.2 Tests with Water Package Accelerated by Piston	12
5.3 Tests with 6.2 kg. Piston Impacting Water Package	12
5.4 General Test Procedures	12
6.0 TEST RESULTS	13
6.1 Gas Gun Calibration	13
6.2 Tests with 3.0 kg Piston Impacting Water Package	13
6.3 Tests with Water Package Accelerated by Piston	18
6.4 Tests with 6.2 kg Piston Impacting Water Package	20
7.0 ANALYSIS OF RESULTS	20
7.1 Method of Calculation	20
7.2 Graphical Results	29
8.0 CONCLUSIONS	31
9.0 RECOMMENDATIONS	32
REFERENCES	33
APPENDIX A - DESIGN OF AMERICAN-MADE NOZZLE	A1

LIST OF FIGURES

	Page
1. Drawing of Pressure Chamber, Adapter and Voitsékhovskiy Nozzle	4
2. Schematic Drawing of Water Jet Test System	5
3. Photograph of Water Jet Test System	6
4. Drawing of 3.0 kg Piston	8
5. Drawing of 6.2 kg Piston	9
6. Schematic Diagram of Instrumentation	11
7. Air Gun Calibration	14
8. Shot #13	15
9. Shot #15	16
10. Shot #16	17
11. Shot #26	19
12. Shot #32	21
13. Shot #33	22
14. Shot #34	23
15. Shot #35	24
16. Shot #36	25
17. Shot #40	26
18. Shot #41	27
19. Specific Energy vs. Specific Pressure for Single Pulse Craters	31
A-1 Drawing of American Design Nozzle	A2

ROCK DISINTEGRATION BY PULSED LIQUID JETS

SUMMARY

Laboratory experiments were conducted to determine the energy required to break three types of rock using pulsed high pressure water jets and to determine the effect of jet stagnation pressure on the efficiency. The pulsed jets were produced using a special nozzle which was imported from Prof. B.V. Voitsekhovskiy at the Institute for Hydrodynamics in Novosibirsk, U.S.S.R. The nozzle has a cross section area which decreases exponentially with length. Water was extruded through the initially empty nozzle by impact of a piston which was fired from a gas gun.

Jet velocities up to 5900 feet per second (1800 m/sec) were obtained which corresponds to a jet stagnation pressure of 234,000 pounds per square inch (1620 MN/m²).

It was found that the energy required per unit volume of rock broken decreases very greatly as the jet pressure is increased from 1.43 to 3.95 times the compressive strength of the rock. A value of specific energy of 500 Joules per cubic centimeter was observed for craters in Barre granite. The only rock disintegration system which has achieved lower energy requirements is the use of mechanical tools such as impact hammers. In many cases, the one foot cubic samples were split or shattered by the water jet pulse.

The trend of the data indicate that lower values of specific energy can be obtained by using jet pressures higher than 234,000 psi. However larger samples and/or in situ testing are required to avoid splitting of the samples and to provide data applicable to tunneling.

With this type of nozzle, there was evidence that the optimum standoff distance from the nozzle to the rock should be quite short (only a few inches) in order to break the rock most effectively.

No significant mechanical damage to the nozzle has been observed after a total of 43 test shots.

A spare nozzle of similar design, but with smaller exit diameter and higher pressure capability is being fabricated in the U.S. and is expected to be completed by the end of March, 1972.

Further testing with both the Russian-made and American-made nozzles is recommended at jet pressures approaching 800,000 psi, using two foot cubic rock samples in order to optimize the rock disintegration process. It is expected that the proposed tests will demonstrate the feasibility of efficient rock disintegration using pulsed water jets. Such tests will supplement but not duplicate tests which may be undertaken in the future by the U.S. Department of Transportation using a larger water cannon.

1.0 OBJECTIVES AND SCOPE

The object of the research program was to optimize the efficiency of rock disintegration by pulsed high pressure water jets. Experiments were conducted on the cratering and splitting of sandstone, limestone and granite by pulsed cumulative water jets with jet velocities up to 5900 ft/sec (1800 m/sec). For water at normal density, this corresponds to a jet stagnation pressure of 1620 MN/m^2 (234,000 psi). The high energy pulsed jets were produced using a Voitsekhovsky-type nozzle (U.S. patent 3,343,794) with a jet diameter of 0.716 cm. The experimental data were correlated in terms of dimensionless parameters. The test objective was to determine the jet parameters which minimize the energy required per unit volume of rock broken.

2.0 INTRODUCTION

Liquid jets are of interest for rock disintegration because:

1. They can break rock by a continuous or quasi-continuous process which is advantageous for mechanization in a rapid excavation system.
2. They can break rock without wearing out tools, thereby permitting a potentially long life tunneling system.
3. The breakage mechanisms are applicable to all types of rock (e.g. not limited to those with certain thermal, chemical or physical characteristics).
4. The use of a liquid helps to minimize dust generation.
5. The use of a liquid minimizes the ignition hazard in an explosive environment (e.g. methane in air).

Since water is the lowest cost liquid available, it is almost universally used for experiments in rock disintegration. However, additives may be introduced to aid in maintaining jet integrity or to assist in lubricating the equipment. Solid abrasives may be added, but they tend to wear out nozzles.

Liquid jets may be either continuous or pulsed. If continuous, they are usually traversed across the rock face to cut one or more slots. If pulsed, one or more pulses may be directed to one location, then the nozzle moved to hit a different location.

Research has been conducted by many investigators on the cutting or fracture of rock by liquid jets. However, there has been insufficient data and inadequate theory to determine the optimum jet parameters. It has been reported that the energy required to break rock by pulsed jets decreases as the jet stagnation pressure increases in the range up to 10 to 20 times the compressive strength. (Ref. 1, 2, 3). However, the values of specific energy reported have varied widely. Therefore a primary objective of this research was to study the effect of jet stagnation pressure on specific energy for pulsed jets of water impinging on samples of three types of rock.

Analysis of existing data (Ref. 4) indicates that pulsed jets are most efficient if the length-to-diameter ratio of the liquid slug is not too large (less than 1000). Therefore the type of nozzle used in this project was one which projects a short duration pulse at very high pressures.

3.0 EXPERIMENTAL EQUIPMENT

It was initially planned to conduct the experiments using a Voitsekhovsky-type nozzle (Ref. 5) which was to be made in the U.S., but of similar design to the nozzles used by Prof. B.V. Voitsekhovsky at the Institute for Hydrodynamics in Novosibirsk, Siberia. The nozzle was designed (See Appendix A and Fig. A-1) and fabrication was initiated by the Speco Division of Kelsey-Hayes Corp. in Springfield, Ohio. However, when it became apparent that there would be a delay in completion, it was decided to purchase a somewhat similar nozzle directly from the U.S.S.R. in order to assure availability for tests during the one year program.

Fig. 1 shows the Russian-made nozzle mounted with an adapter to the pressure chamber which was made by Kelsey-Hayes. The tests were conducted by extruding a volume of water through the nozzle by means of a piston which was accelerated by nitrogen in a gas gun. Fig. 2 shows a schematic drawing of the water jet test system and Fig. 3 shows a photograph of the actual installation.

In general, a Voitsekhovsky type nozzle has a cross-section area which decreases exponentially with length. It is filled with air or vacuum prior to a shot. A free piston impacts a volume of liquid and extrudes it through the nozzle. The shape of the nozzle causes unsteady acceleration of water as the nozzle fills, which results in accumulation of kinetic energy in the leading part of the jet, at the expense of kinetic energy of the larger mass of water near the nozzle entrance. This is an example of a "cumulation" process. At the instant when the nozzle is completely filled, the piston velocity is quite low and most of the piston energy is converted to kinetic energy of water in the nozzle. In fact a large fraction of the kinetic energy is in the final sections of the nozzle where the velocities are very high. The jet pulse has a high initial velocity, followed by a decay of jet velocity, with a total time duration of about 1 to 2 msec.

Based on a simplified analysis of incompressible liquid flow through an exponential nozzle, it can be shown that the entrance chamber pressure should remain constant during the piston deceleration if the following relationship of parameters is satisfied:

$$K = \frac{S_0 M}{\rho S_1^2} \quad (1)$$

where K = the nozzle construction parameter, which is the length over which the area decreases by a factor of e

M = Mass of the piston

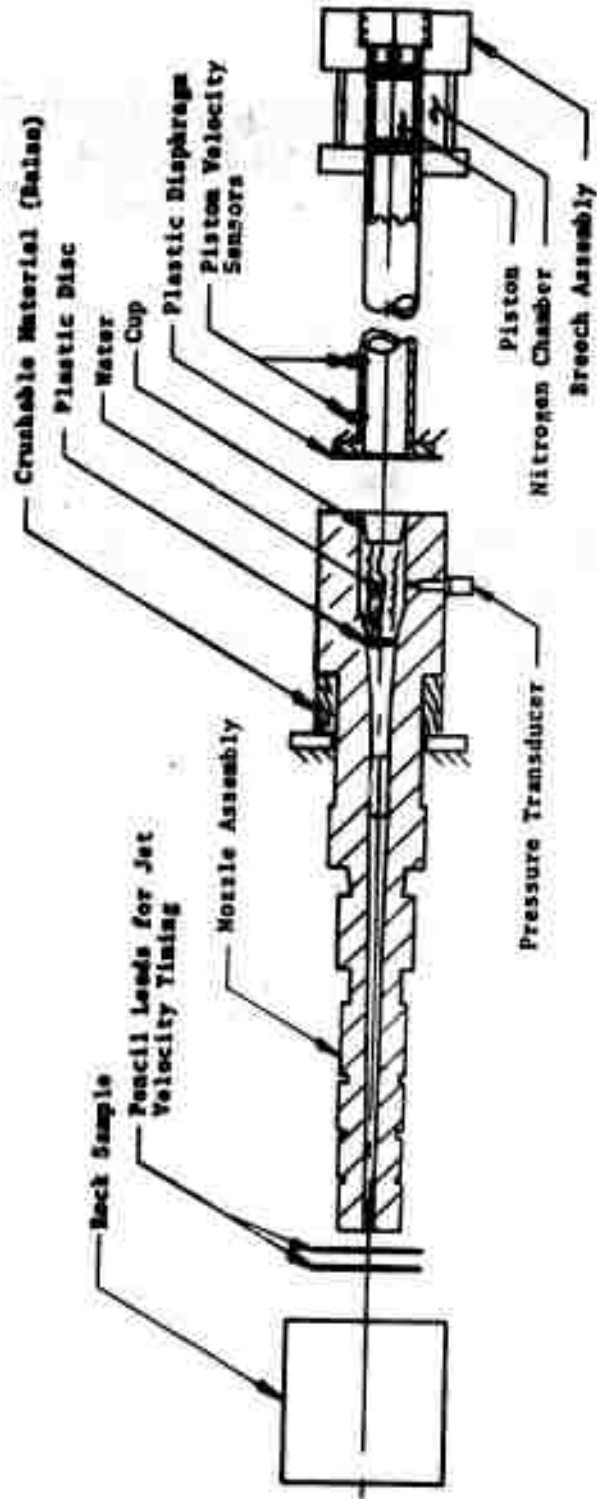


Fig. 2 Schematic Drawing of Water Jet Test System

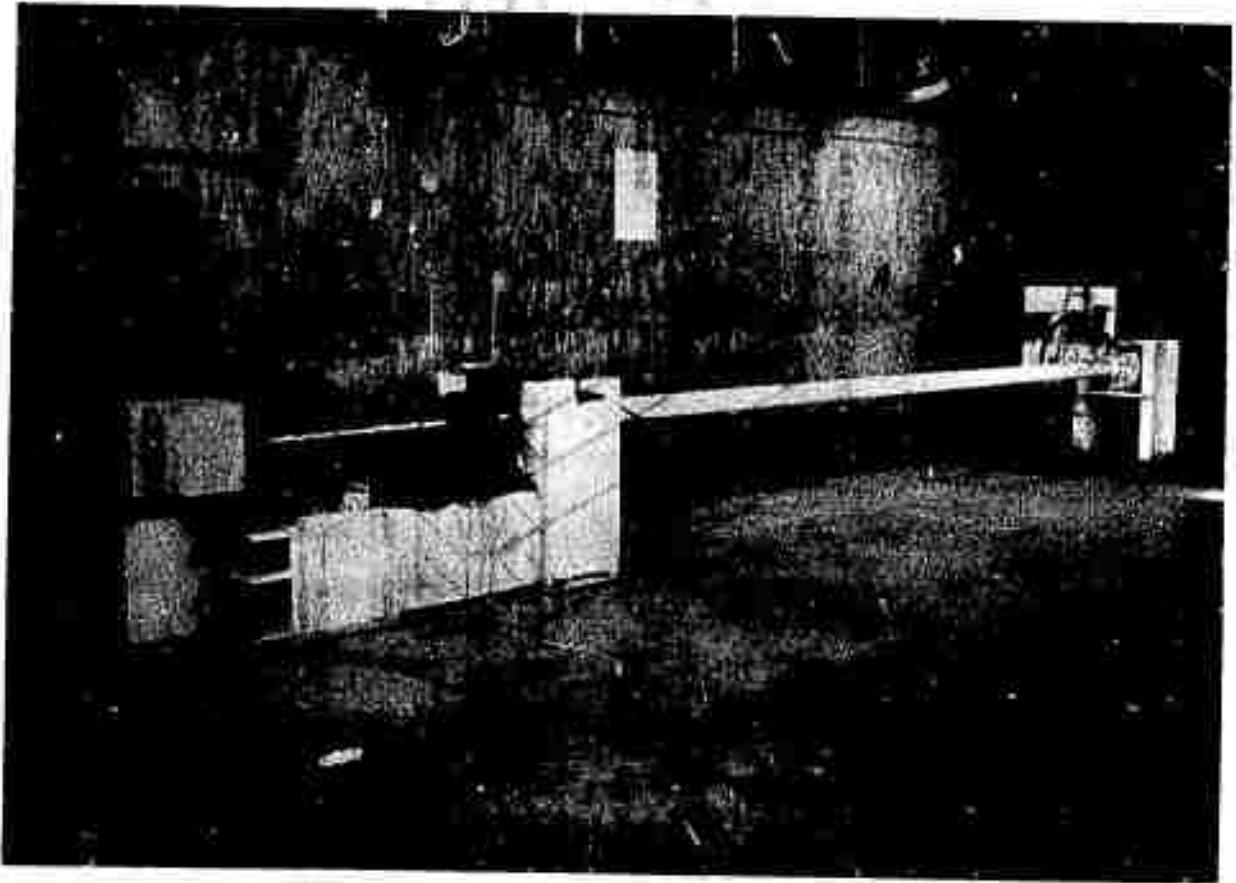


Fig. 3 Photograph of Water Jet Test System

S_0 = entrance area of the nozzle

S_1 = piston cross-section area

ρ = density of liquid

It is desirable for the chamber pressure to remain constant during the stroke in order to maximize the efficiency of energy transfer to the water for a fixed limit on the design pressure of the pressure chamber.

In the actual nozzle system, (Fig. 1) the pressure chamber was 8.36 cm in diameter by 18 cm long. The nozzle entrance diameter was 5.4 cm and the exit diameter was 0.716 cm. Except for a 9.15 cm long adapter section having a constant diameter of 3.2 cm, the nozzle area decreased approximately exponentially with length from the 5.4 cm diameter throat to the 0.705 cm diameter. The adapter was necessary to mate the metric thread of the Russian nozzle to the thread of the American-made pressure chamber which had been designed to fit the American-made nozzle. The resulting deviation of the shape from a true exponential undoubtedly modifies the nozzle performance somewhat. The nozzle construction parameter, K , had a value of 22.5 cm. An exit collimator with an entrance diameter of 0.714 cm, exit diameter of 0.716 cm, and length of 5 cm was used. The volume of the nozzle from the throat to the exit was 560 cm³. The nozzle was made in sections using double-walled alloy steel construction, with the inner sleeves in compression to sustain maximum nozzle wall pressure up to 1250 MN/m² (180,000 psi) in the regions of maximum wall pressure near the exit. The pistons were accelerated by compressed nitrogen in a gas gun of 8.25 cm bore and 5 meters length. Each piston had two neoprene O-rings which were lubricated to decrease sliding friction. The gas gun barrel was generally closed at the exit end by a thin plastic diaphragm and was evacuated to a barrel pressure of about 20 Torr before each shot in order to increase gun performance, and to prevent a jet of gas from impinging on the water package prior to impact. The piston would shear the plastic and continue in free flight for approximately 20 cm. before impacting the enclosed volume of water in the pressure chamber. The O-rings were only relied on for sealing gaseous nitrogen during the acceleration in the gun barrel, because they were generally extruded and expelled during water impact.

The theoretically correct piston mass to satisfy Eq. 1 was 2.8 kg. Initial experiments were conducted using hardened steel pistons of 8.25 cm diameter weighing 3.0 kg (See Fig. 4). However, it was found that water leakage through the 0.05 cm radial clearance around the piston dissipated a part of the piston kinetic energy. Therefore piston weight was later increased in test shot #32 to 6.2 kg (See Fig. 5) to compensate

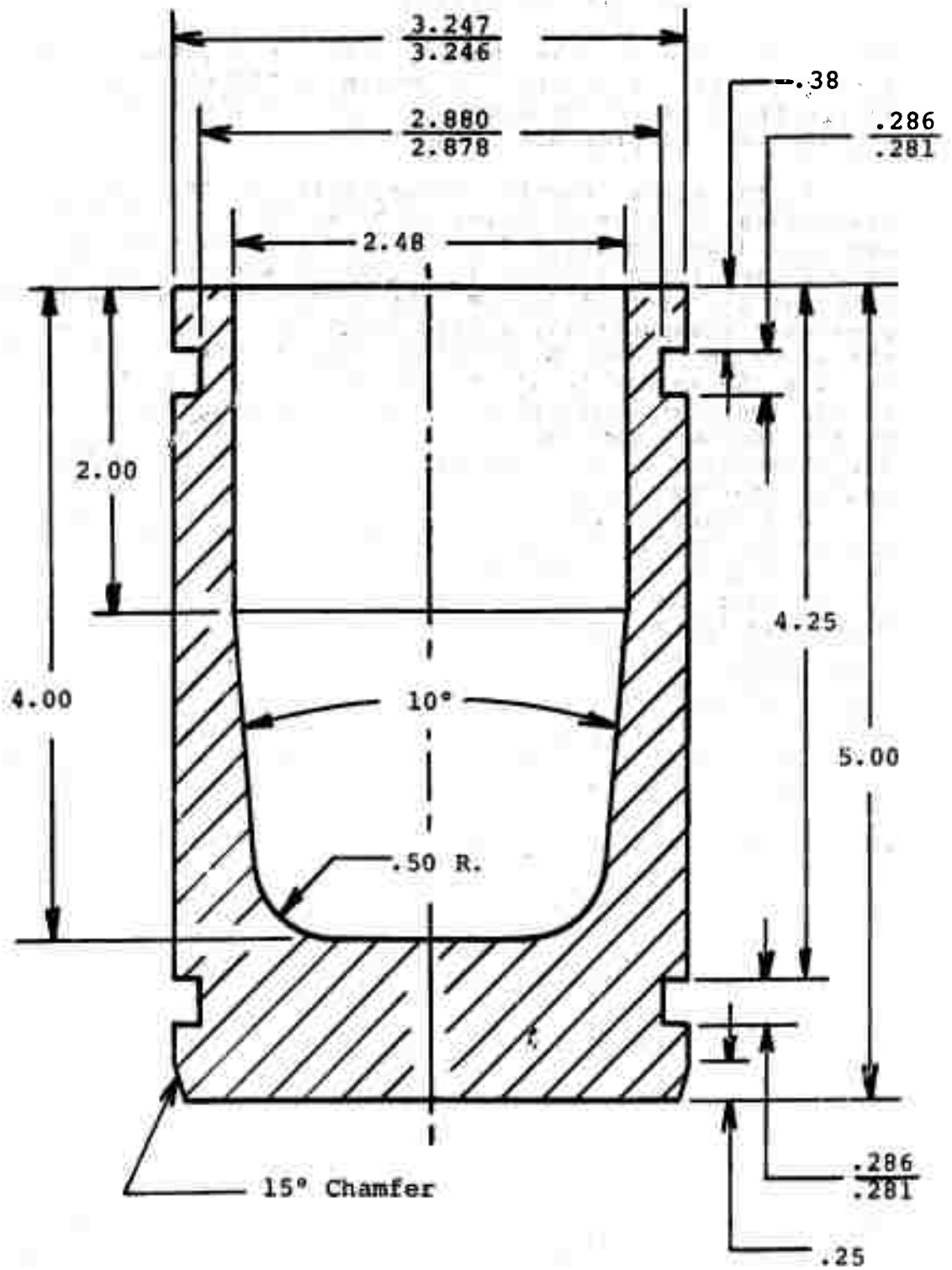


Fig. 4 Drawing of 3.0 Kg Piston

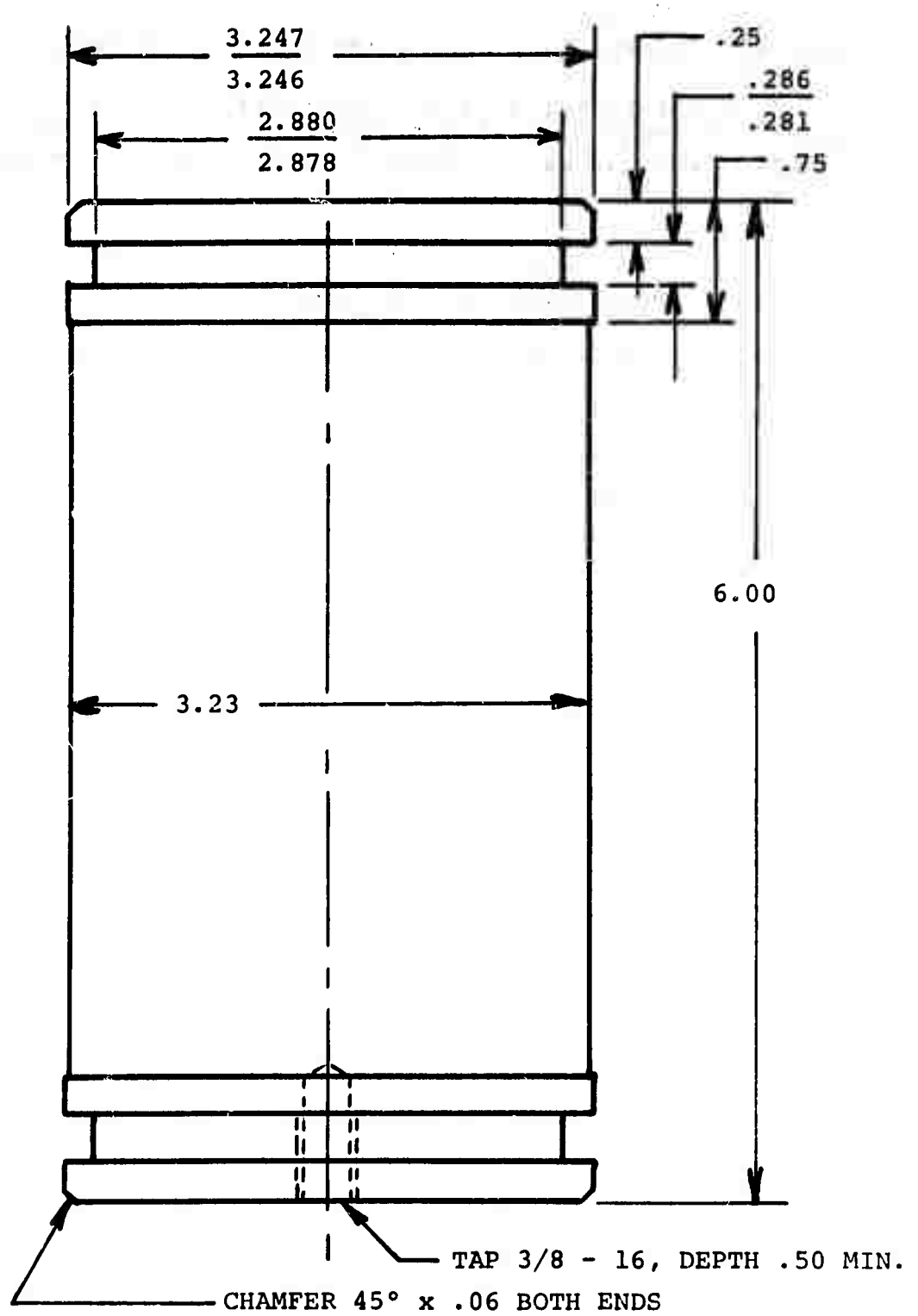


Fig. 5 Drawing of 6.2 Kg Piston

for this energy loss during the extrusion stroke.

In all tests, a 30 cm cubic rock sample was located with its front face at a distance of 7.5 to 27 cm from the nozzle exit and was centered on and normal to the nozzle axis.

4.0 INSTRUMENTATION

4.1 Piston Velocity Measurement

A schematic diagram of the instrumentation system is shown in Fig. 6. The piston kinetic energy for each shot was determined by measuring the velocity of the piston at the exit from the gas gun barrel. The piston velocity sensors were two wire probes located a distance of 12 cm apart. The tips of the wire probes extended radially into the gun barrel so that the two wires were successively shorted to ground when the piston passed.

The electrical pulse from the first probe was used to trigger the sweep of a Tektronix Model 502A dual beam oscilloscope. The pulse from the second probe was displayed on the upper trace of the oscilloscope. The trace was photographed with a Polaroid oscilloscope record camera. The time between the start of the sweep and the appearance of the pulse from the second probe was measured on the oscillogram to determine transit time of the piston over the 12 cm distance. Piston velocities were varied from 105 to 210 m/sec. with the 3.0 kg pistons and from 121 to 135 m/sec with the 6.2 kg pistons.

4.2 Chamber Pressure Measurement

The pressure at the nozzle entrance was recorded using a Kistler Model 207C3 pressure transducer with a Model 549 battery coupler and a 24 volt dry cell battery. The output was recorded on the lower trace of the oscilloscope. Based on the transducer calibration, the pressure amplitude was 261 MN/m² per centimeter of vertical displacement on the oscilloscope. The 0.31 cm diameter hole leading to the transducer was located in the pressure chamber at a distance of 6.3 cm from the start of the nozzle convergence. It was filled with a rod of neoprene in an attempt to damp sharp pressure spikes which might damage the transducer.

4.3 Jet Velocity Measurement

The initial velocity of the water jet as it left the nozzle was measured by recording the time between breakage of two pencil leads located transversely across the jet axis. The first lead was generally located a distance of 3.05 cm from the nozzle exit and the spacing between leads was 3.05 cm

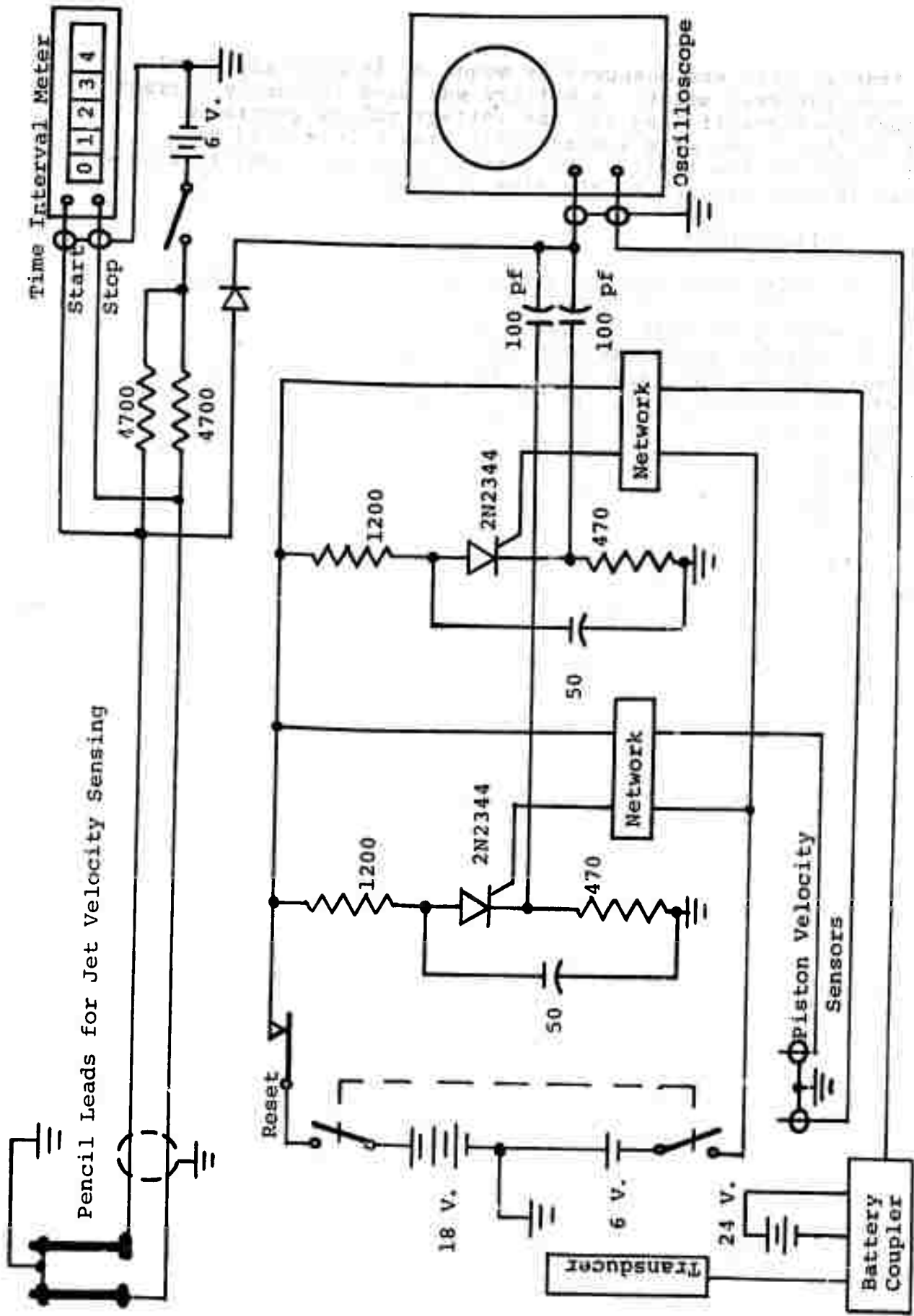


Fig. 6 Schematic Diagram of Instrumentation

The transit time was measured by means of an Eldorado Model 255 time interval meter. A battery was used to supply current through each pencil lead and the voltage pulses generated when the two leads were successively broken were used to start and stop the timer. The transit time was visually displayed in microseconds by the time interval meter.

5.0 TEST PROCEDURES

5.1 Tests with 3.0 kg Piston Impacting Water Package

In tests 1 through 20, the 3.0 kg pistons were used (Fig. 4) and the water was initially located within the pressure chamber for each shot. Tests were made with a variety of configurations for the water package and with both air and vacuum in the gas gun barrel. Best results were achieved in shots with vacuum in the gun barrel. This was achieved by sealing a plastic diaphragm to the barrel exit and using a vacuum pump to produce a pressure of about 20 Torr in the barrel. The primary purpose of the vacuum in the barrel was to prevent ejecting a jet of air ahead of the piston which could disturb the water package prior to impact. A secondary benefit was the slightly higher piston velocity achievable for a given nitrogen pressure.

5.2 Tests with Water Package Accelerated by the Piston

In tests 21 through 31, the light weight (3.0 kg) pistons were used, but the water was packaged in a plastic cylinder or rubber balloon and accelerated in the gun barrel ahead of the piston. The purpose was to reduce the amplitude of the sharp pressure spikes which were produced when the piston hit water. However, because of inconsistent test results, this technique was abandoned.

5.3 Tests with 6.2 kg Piston Impacting Water Package

In tests 32 through 43, the heavier pistons (6.2kg) as shown in Fig. 5 were used and the water was initially located within the pressure chamber. In these shots a vacuum was always used in the gun barrel.

5.4 General Test Procedures

For tests with air in the nozzle, a 0.32 cm thick styrofoam disc was located at the nozzle throat (at a diameter of 5.4 cm) and a plastic cup with about 0.1 cm wall thickness was located at the entrance to the 8.35 cm diameter pressure chamber. The space between these closures was filled with a volume of approximately 890 cc of tap water. The bottom of the plastic cup was located about 5 cm inside the chamber entrance in order to reduce the water volume to 1.6 times

the volume of the nozzle. Therefore a volume of about 275 cm of ambient air was initially trapped by the piston as it entered the pressure chamber.

For tests with vacuum in the nozzle, it was found that the styrofoam disc at the nozzle throat would not withstand the vacuum. Therefore it was replaced in these cases (Tests 38, 39, 42, and 43) by a disc of polystyrene of 0.8 mm thickness, which was pressed into the nozzle throat and sealed with vacuum grease.

To conduct a test, a piston was loaded into the breech of the gas gun and a plastic diaphragm was sealed across the gun barrel exit. A vacuum was pulled on the gun barrel and the space behind the piston. The annular nitrogen chamber of the gas gun was loaded with compressed nitrogen at a pressure up to 5.53 MN/m^2 (800 psi). Firing of the piston was initiated by opening a solenoid valve which applied pressure to the rear face of the piston, moving it past ports in the barrel which admitted nitrogen gas from the annular chamber to accelerate the piston.

After each test shot, the rock sample was photographed and the volume of rock broken was measured. The transit time from the jet velocity meter was recorded and the oscillogram analyzed.

6.0 TEST RESULTS

6.1 Gas Gun Calibration

Before conducting water jet tests, calibration shots of the 3.0 kg pistons were conducted in order to determine the nitrogen chamber pressure needed. Attempts to use Teflon O-rings on the piston were unsuccessful because the rings failed to seal. Therefore Neoprene or Buna-N O-rings were used.

Fig. 7 shows a plot of piston velocity as a function of nitrogen pressure. The initial calibration tests were not extended beyond a pressure of 300 psi because the pistons were not easily stopped by styrofoam energy absorbing material. Also shown in Fig. 7 are the data for both the 3.0 and 6.2 kg pistons when fired in actual water jet tests.

6.2 Tests with 3.0 kg Piston Impacting Water Package

Figures 8, 9, and 10 show the test results for shots 13, 15, 16. The upper half of each figure is a photograph of the rock sample after the test and the lower half is the oscillogram record. The oscillogram for each test shows on the upper trace the pulse indicating the piston transit time over the 12 cm spacing between the two sensors at the end of the gun barrel. On the lower trace is recorded the output of

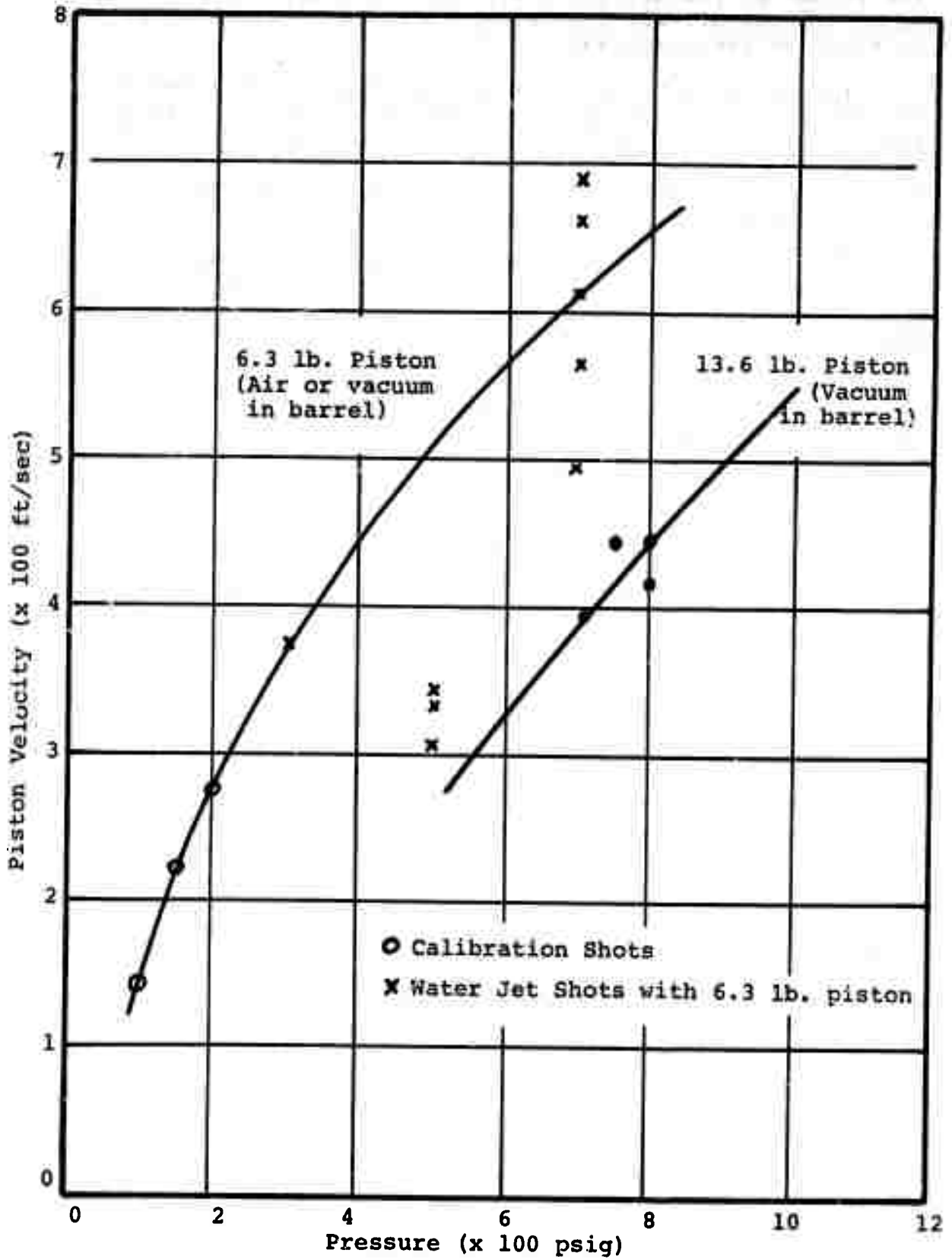


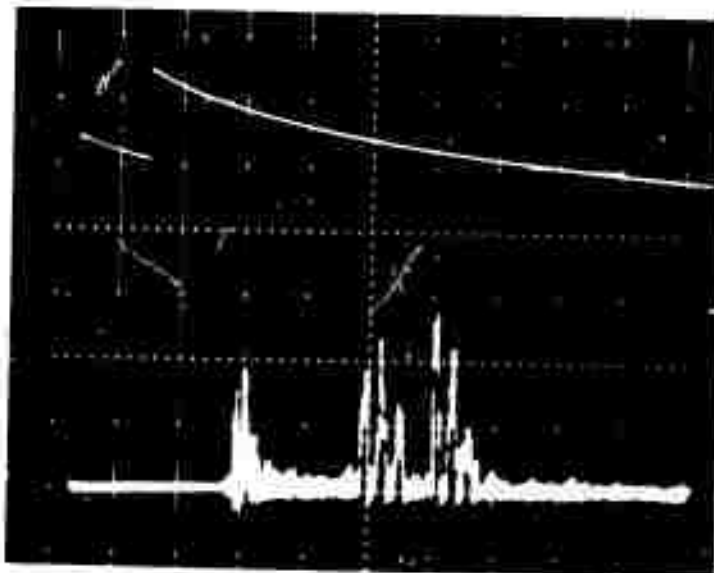
Fig. 7 Air Gun Calibration



Reproduced from
best available copy.

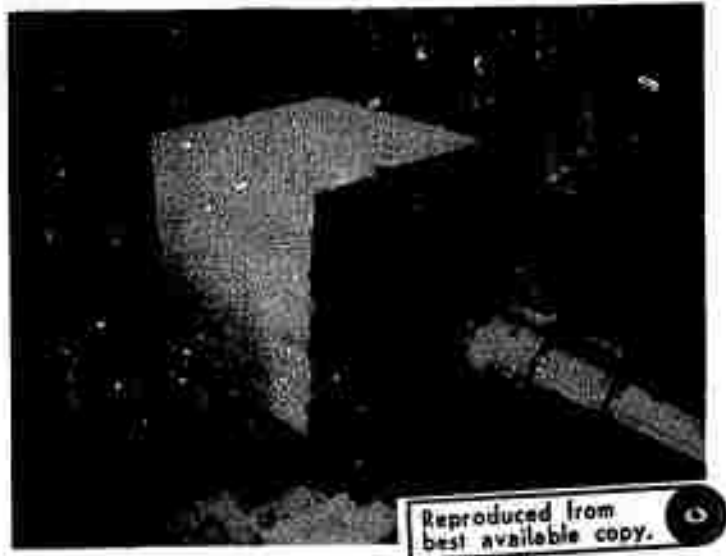


Shot #13
Fracture of Berea Sandstone
Piston Energy = 45,000 ft-lbs (61,000 J.)
Crater Volume = 260 cc
Volume broken off = 3000 cc

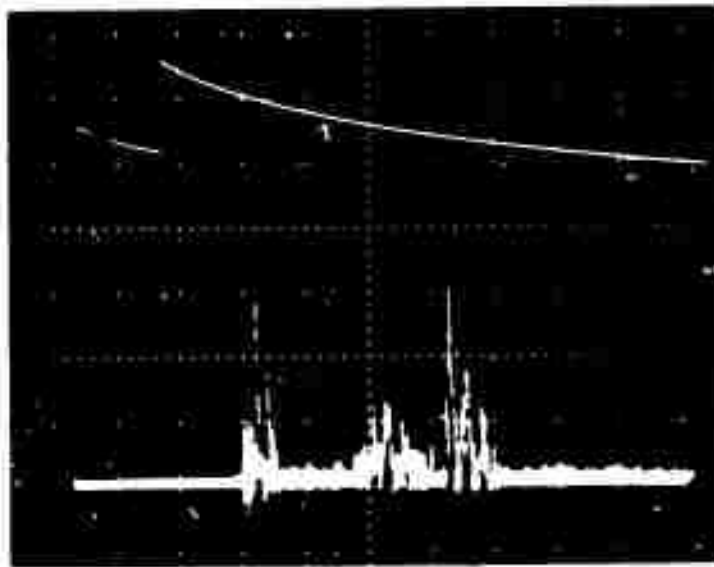


Sweep speed = 0.5 msec/cm
Pressure amplitude = 37,800 psi/cm
Peak chamber pressure = 100,000 psi

Fig. 8



Shot #15
Crater in Barre Granite
Piston Energy = 33,000 ft-lbs (45,000 J.)
Crater Volume = 33 cc
Specific energy = 1360 J/cc

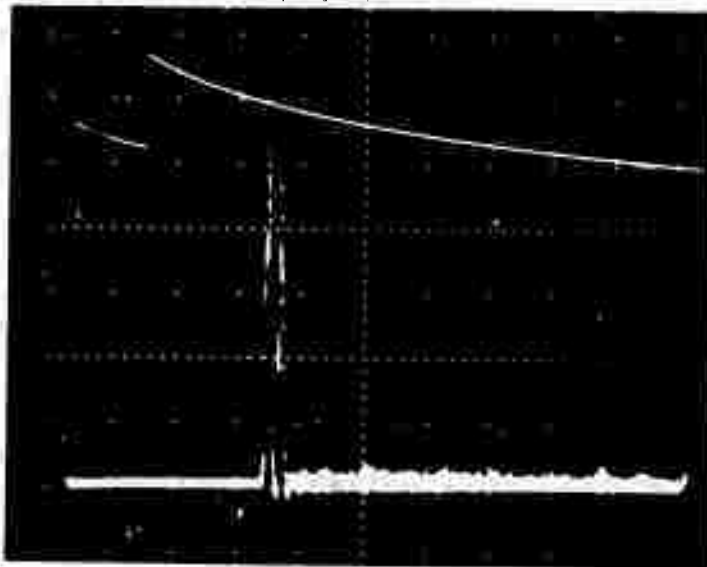


Sweep speed = 0.5 msec/cm
Pressure amplitude = 37,800 psi/cm
Peak chamber pressure = 113,000 psi

Fig. 9



Shot #16
Fracture of Indiana limestone
(Jet perpendicular to lamination)
Piston energy = 48,000 ft-lbs (65,000 J.)
Volume broken off = 2400 cc



Sweep speed = 0.5 msec/cm
Pressure amplitude = 37,800 psi/cm
Peak chamber pressure = 197,000 psi

Fig. 10

the chamber pressure transducer.

Figure 9 shows the typical rock failure mode consisting of an approximately conical spall crater in the face of the rock. Figures 8 and 10 show the results of extensive splitting of the rock which is the result of fractures initiated at the jet crater which extend to the free surfaces of the sample. On each figure is recorded the piston energy and the rock volume removed.

The pressure traces in the oscillograms of Fig. 8, 9, and 10 show that the initial pressure pulse typically consists of a group of two or more sharp pressure spikes with a total duration of the order of 0.3 msec. The first pressure spike is caused by the shock wave generated when the piston hits the water. The second pressure spike usually occurs with a short delay time of about 0.1 msec and is believed to be caused by the first vibration of the piston in the axial mode. After this first group of pulses in Fig 8 and 9, there is a period of about 0.7 msec. with low or zero pressure, during which the piston must have lost contact with the water. Then a series of pressure pulses ensue which may continue for 1.0 msec which occur while the nozzle is becoming filled with water. These delayed pulses are caused by the piston catching up with the water interface, making multiple piston impacts accompanied by piston vibration. In Fig. 10, there is no evidence of the delayed pressure pulses, but the amplitude of the pressure spikes was nearly 200,000 psi. These high pressures greatly exceeded the nominal rating of the pressure transducer (100,000 psi) and the design pressure of the pressure chamber (100,000 psi). Therefore, beginning with shot #21, attempts were made to reduce the amplitude of these high pressure spikes in order to avoid damage to the transducer or chamber.

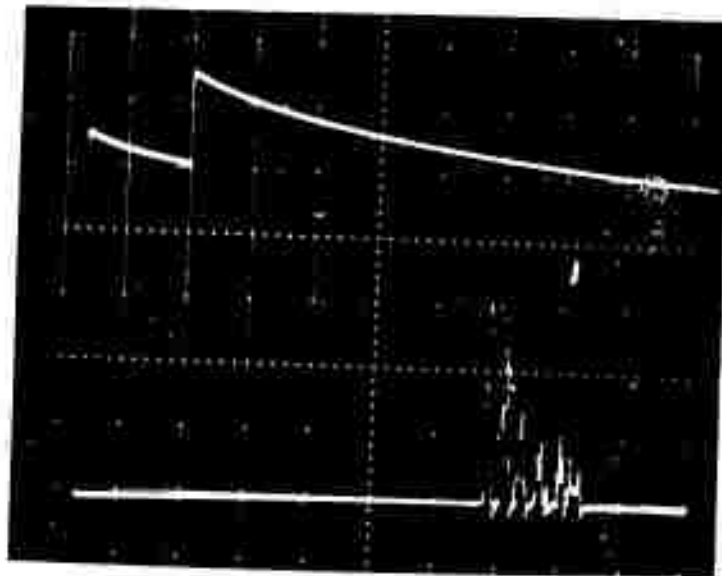
6.3 Tests with Water Package Accelerated by Piston

Since the high pressure spikes were caused by shock waves associated with the high velocity impact of the piston against water, shots 21 through 31 were made with packages of water which were accelerated by the piston in the gun barrel.

Fig. 11 shows the results of one successful shot of this type. In this case, a one pint plastic jar of water, preceded by a balloon filled with one pint of water were loaded ahead of the piston. A vacuum was pulled in the gun barrel and the water and piston were fired into the empty pressure chamber. It is seen that the initial pressure amplitude was only 121,000 psi. The rapid drop in pressure on successive piston vibrations indicates that the piston was losing velocity rapidly, probably at the expense of wasted energy due to water leakage past the piston. This indicated that the piston mass should be increased to compensate for leakage.



Shot #26
Crater in Berea sandstone
Piston energy = 22,000 ft-lbs (30,000 J.)
Crater volume = 72 cc
Specific energy = 415 J./cc



Sweep speed = 0.5 msec/cm
Pressure amplitude = 37,800 psi/cm
Peak chamber pressure = 121,000 psi

Fig. 11

Most of the shots 21 through 31 gave erratic results. Only three of the eleven shots resulted in appreciable rock cratering. It was concluded that the water packages were probably not surviving the acceleration by the piston, but were breaking and allowing water to be dispersed in air ahead of the piston. Therefore it was decided to return to the original method, but to use the heavier pistons. They would permit a lower impact velocity and lower amplitude pressure spikes for a given energy, but also provide extra kinetic energy to allow for piston leakage.

6.4 Tests with 6.2 kg Piston Impacting Water Package

Test shots 32 through 43 were made with the heavier pistons. Figures 12 through 18 show the results for the successful tests made with ambient air pressure in the nozzle. (The pressure trace in Fig. 14 is invalid because of a bad connection in the electrical circuit.)

It is seen that there is considerable variability in the type of pressure pulse and also in the extent of rock damage, even though all seven shots were made at approximately the same piston velocity of 121 m/sec (396 ft/sec). However, the pressure pulse generally consists of an initial cluster of closely spaced spikes (0.2 to 0.3 msec long), followed by a delay of at least 0.5 msec, then usually a series of additional pressure spikes which occur during the time that the nozzle is filling with water.

Fig. 12 and 16 show typical spall craters. Fig. 13, 14, 15, 17 and 18 show extensive splitting or shattering of the rock samples.

7.0 ANALYSIS OF RESULTS

7.1 Method of Calculation

Specific energy was calculated by dividing the piston kinetic energy by the volume of the spall crater in the face of the sample. No correction was made for the energy loss by leakage past the piston. Specific pressure was calculated as the ratio of the initial jet stagnation pressure q to the compressive strength of the rock.

The jet stagnation pressure was calculated using the equation:

$$q = \frac{\rho V_j^2}{2}$$

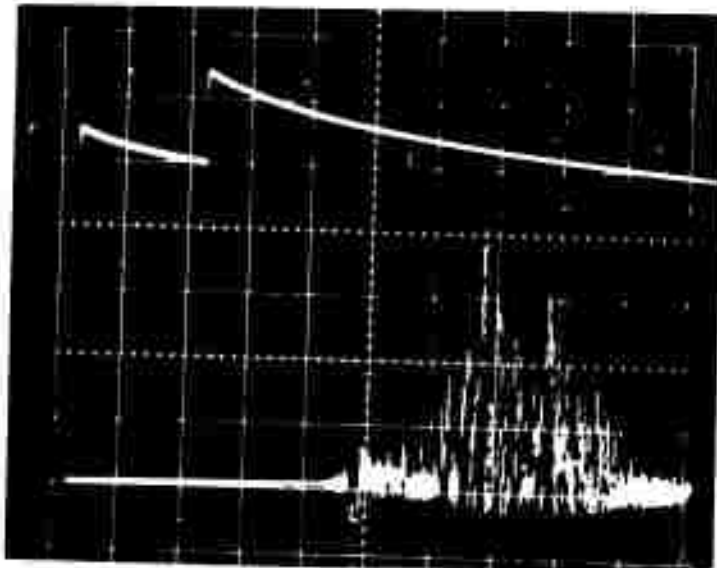
where V_j = jet velocity measured by the time between breaking of pencil leads.

ρ = density of water, assumed to be 1 gm/cm³.

Table 1 shows a summary of all the test data for which jet velocity measurements were obtained. The data are grouped



Shot #32
Crater in Berea sandstone
Piston energy = 33,000 ft-lbs (45,000 J.)
Crater volume = 165 cc
Specific energy = 270 J/cc

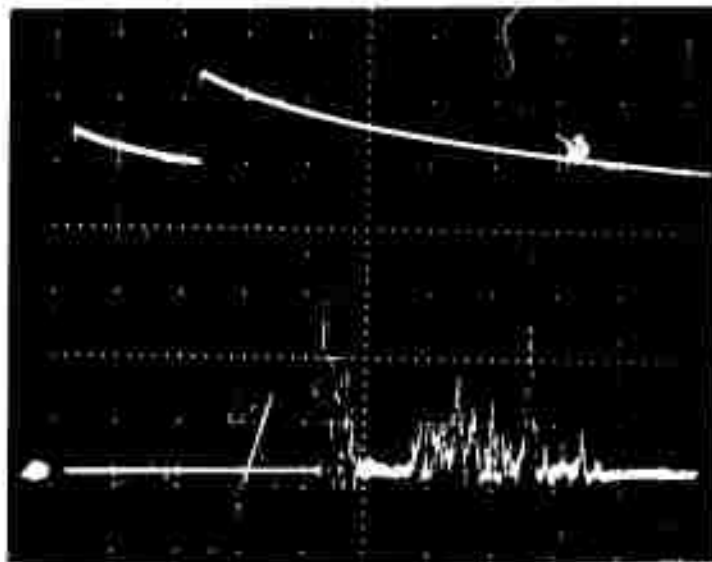


Sweep speed = 0.5 msec/cm
Pressure amplitude = 37,800 psi/cm
Peak chamber pressure = 151,000 psi

Fig. 12



Shot #33
Fracture of Indiana limestone
(Jet parallel to laminations)
Piston energy = 33,000 ft-lbs (45,000 J.)
Volume broken off = 4600 cc



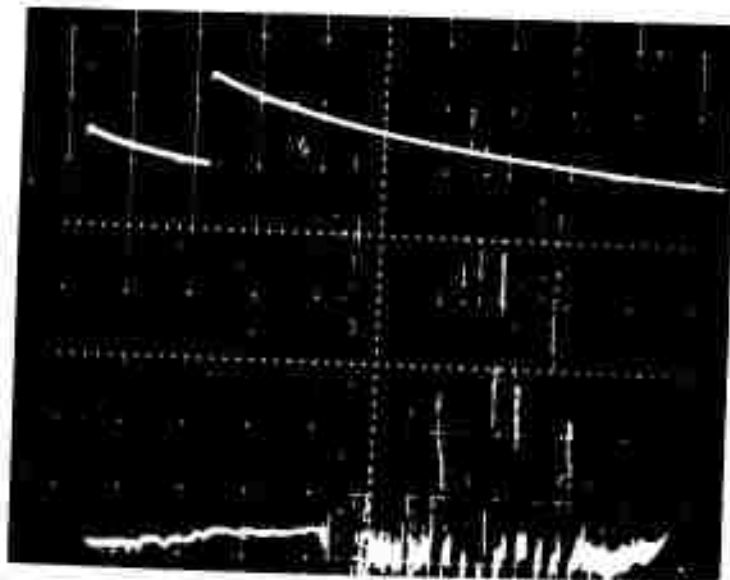
Sweep speed = 0.5 msec/cm
Pressure amplitude = 37,800 psi/cm
Peak chamber pressure = 151,000 psi

Fig. 13



Reproduced from
best available copy.

Shot #34
Fracture of Barre Granite
Piston energy = 33,000 ft-lbs (45,000 J.)
Volume broken off = 2600 cc

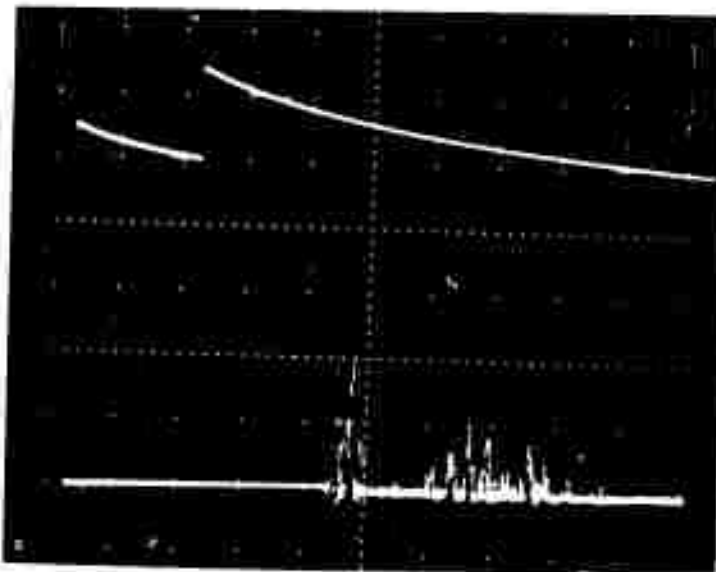


Sweep speed = 0.5 msec/cm
Pressure amplitude = 37,800 psi/cm

Fig. 14

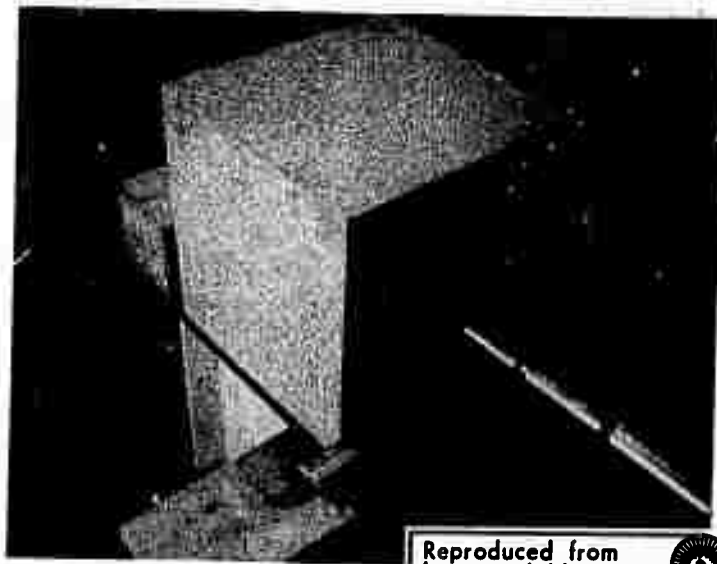


Shot #35
Fracture of Indiana limestone
(Jet perpendicular to lamination)
Piston energy = 33,000 ft-lbs (45,000 J)
Volume broken off = 10,000 cc



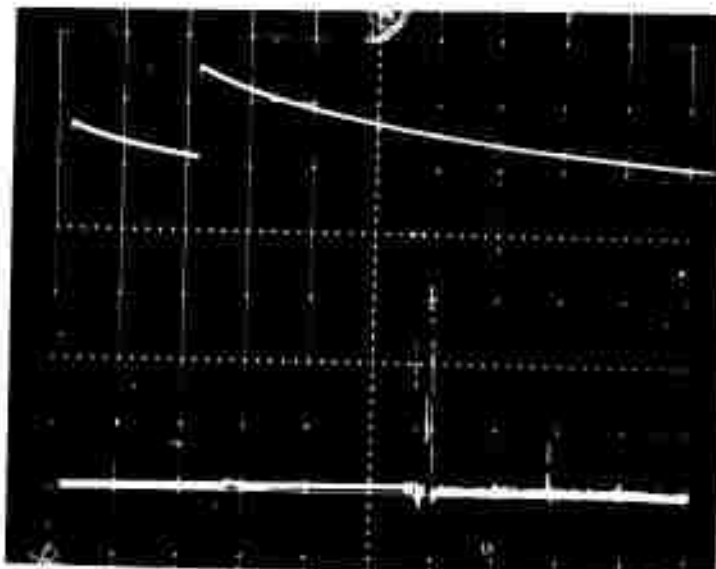
Sweep speed = 0.5 msec/cm
Pressure amplitude = 37,800 psi/cm
Peak chamber pressure = 83,000 psi

Fig. 15



Reproduced from
best available copy. 

Shot #36
Crater in Barre Granite
Piston energy = 33,000 ft-lbs. (45,000 J.)
Crater volume = 90 cc
Specific energy = 500 J/cc



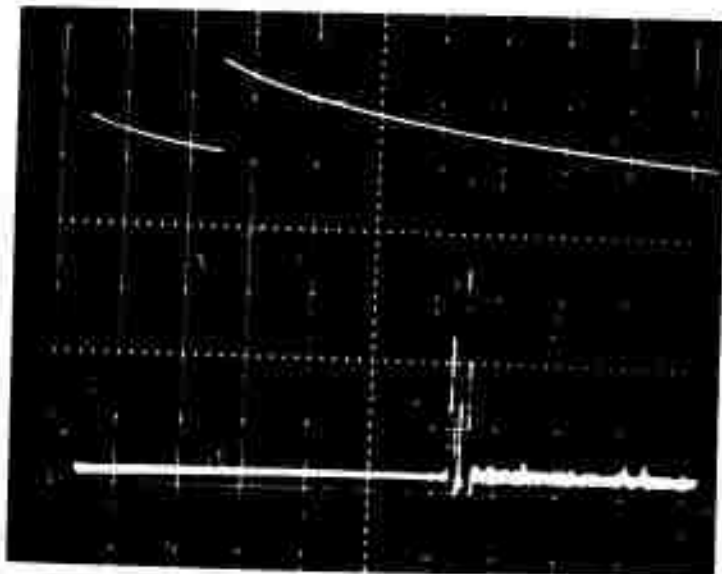
Sweep speed = 0.5 msec/cm
Pressure amplitude = 37,800 psi/cm
Peak chamber pressure = 125,000 psi

Fig. 16

Reproduced from
best available copy.

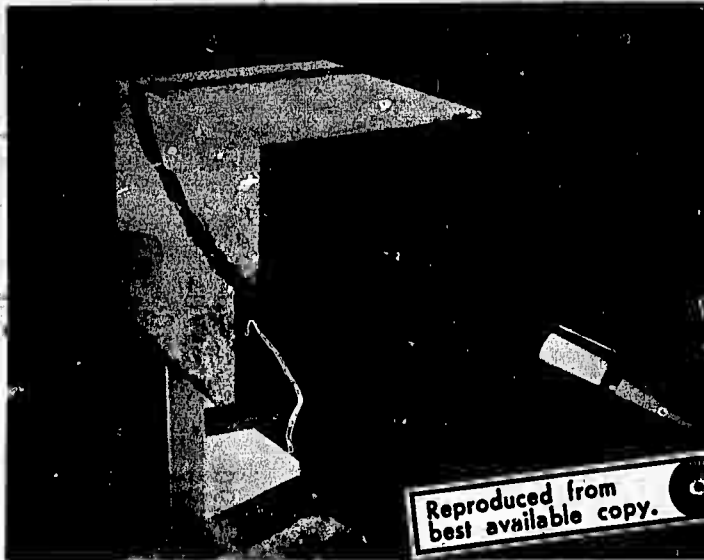


Shot #40
Fracture of Barre Granite, Standoff = 6"
Piston Energy = 33,000 ft. lbs. (45,000 J.)
Volume broken off = 3500 cc

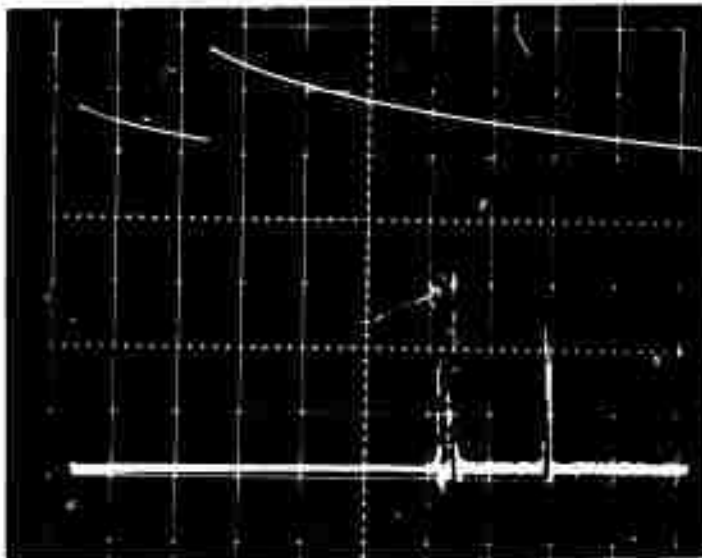


Sweep speed = 0.5 msec/cm
Pressure amplitude = 37,800 psi/cm
Peak chamber pressure = 170,000 psi

Fig. 17



Shot #41
Fracture of Barre Granite, Standoff = 6"
Piston Energy = 33,000 ft. lbs. (45,000 J.)
Volume broken off = 6000 cc.



Sweep speed = 0.5 msec/cm
Pressure amplitude = 37,800 psi/cm
Peak chamber pressure = 113,000 psi

Fig. 18

TABLE 1 - SUMMARY OF TEST DATA

ROCK TYPE	TEST SHOT NO.	PRESSURE IN NOZZLE	STANDOFF DIST. (cm)	PISTON ENERGY (10 ³ JOULES)	CRATER VOLUME (cm ³)	SPECIFIC ENERGY (J/cm ³)	JET VEL. (m/sec.)	JET STAG. PRESS. (MN/m ²)	ROCK COMP. STRENGTH (MN/m ²)	SPECIFIC PRESSURE
BEREA SANDSTONE	6	1 Atm.	20	15.7	25	630	600	190	66	2.88
"	13	1 Atm.	20	58	3000*	20*	420	100	"	1.52
"	32	1 Atm.	20	45	165	273	725	260	"	3.95
INDIANA LIMESTONE (PARALLEL TO LAM.)	14	1 Atm.	20	43	79	545	?	--	73	--
"	17	1 Atm.	20	58	13.5	4300	1130	630	"	8.6
"	33	1 Atm.	15	45	4600*	9.8*	2770 (?)	3800 (?)	"	52 (?)
INDIANA LIMESTONE (PERPEND. TO LAM.)	16	1 Atm.	20	63	2400*	26*	1160	660	"	9.1
"	35	1 Atm.	15	45	10,000*	4.5*	1450	1050	"	14.4
BARRE GRANITE	15	1 Atm.	20	43	40	1070	890	390	210	1.85
"	18	1 Atm.	27	49.5	Negligible		590	170	"	0.82
"	19	"	15	50	0.4	1.25x10 ⁵	780	300	"	1.43
"	34	"	15	45	2600*	17*	925	420	"	2.0
"	36	"	7.5	45	90	500	1050	550	"	2.6
"	37	"	15	45	120	373	765 (?)	290 (?)	"	1.37 (?)
"	40	1 Atm.	15	45	3500*	13*	?	--	"	--
"	41	1 Atm.	15	45	6000*	7.5*	1100	600	"	2.85
"	44	1 Atm.	15	58	820*	71*	1130	625	"	3.0
BARRE GRANITE (VACUUM IN NOZZLE)	39	16 Torr.	15	45	90	500	1390	950	"	4.5
"	42	15 Torr.	15	58	12	4830	1600	1270	"	6.0
"	43	13 Torr.	15	50	15	3330	1800	1600	"	7.6

*SPLIT OFF FROM ROCK SAMPLE

by rock type. Data for limestone are grouped depending on whether the jet direction was parallel or perpendicular to the laminations (bedding planes). The unusually high jet velocity recorded for shot #33 is believed to be invalid.

All data reported in Table 1 except for test shots 39, 42, and 43, were obtained with the nozzle initially filled with air at ambient pressure from the throat section (5.4 cm diameter) to the exit. The throat closure consisted of a disc of low density styrofoam of 0.32 mm thickness. This disc was extruded by the water and caused a bright visible flash at the nozzle exit due to burning in hot compressed air in the nozzle. It is possible that the density of the first few centimeters of length of the jet may have been lower than normal water density because of interface mixing of water with air in the nozzle. Therefore the values of q calculated may be on the high side.

The values of compressive strength σ_c for the sandstone and limestone were measured by compressive crushing of 10 cm cubic samples obtained from the same source as the 30 cm cubic samples. The results were:

Berea sandstone - 66 MN/m²

Indiana limestone - 73 MN/m²

The compressive strength of the Barre granite exceeded the capacity of the testing machine available (171 MN/m²). Therefore, a compressive strength of 210 MN/m² was assumed in the analysis, based on measurements by other investigators.

7.2 Graphical Results

A curve of specific energy is plotted against specific pressure in Fig. 19 for seven test shots against granite and sandstone in which only a spall crater was formed, without fracturing to the edge of the 30 cm square sample. These data are believed to be applicable to the case of a semi-infinite rock sample. The test points include shots at three standoff distances of 7.5, 15, and 20 cm, since there were insufficient tests to separate out the effect of standoff distance on specific energy. It was observed that the jet was relatively ineffective for one test against granite at low jet stagnation pressure (170 MN/m²) at a standoff distance of 27 cm.

The curve drawn in Fig. 19 indicates that the specific energy drops by nearly three orders of magnitude as the specific pressure increases from 1.43 to 3.95. This is no doubt due to a change in the failure mode from granular erosion to shear fractures which form spall craters, breaking out large pieces of rock.

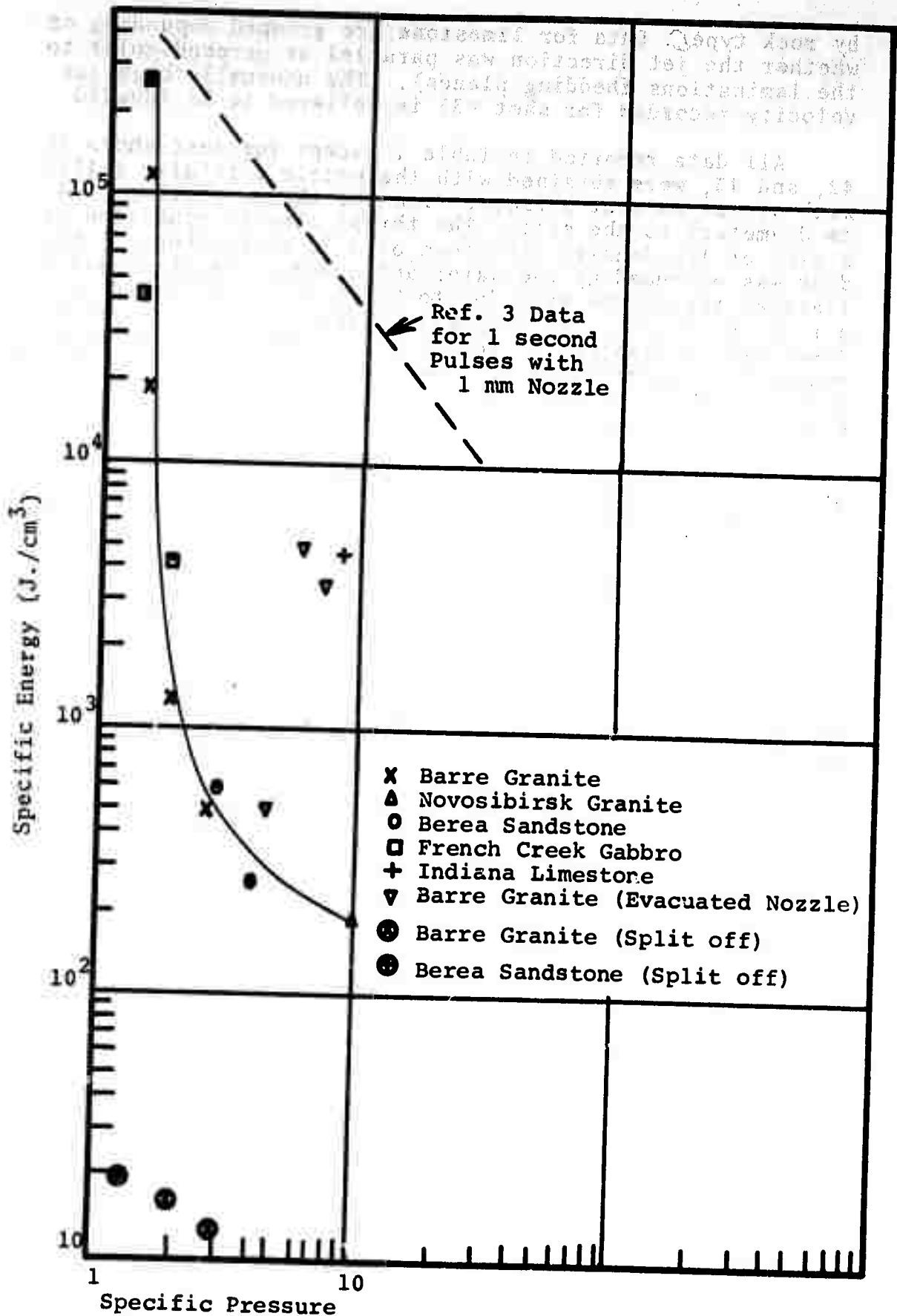


Fig. 19 Specific Energy vs. Specific Pressure for Single Pulse Craters

Also shown is the point representing Voitsekhovskiy's results for single shots with a similar nozzle against granite in a Novosibirsk quarry (Ref. 6). It is seen that the steeply dropping specific energy curve decreases in slope in the range of specific pressures from 3 to 10.

In Fig. 19 are also plotted three test points which were reported by Huck and Singh (Ref. 3) for French Creek Gabbro, being cratered by a 1mm diameter water jet of more than one second duration. (Compared to about 1.5 milliseconds in our case). It is perhaps not coincidental that these points fall on the curve in Fig. 19, since gabbro spalls quite easily with a shallow cone angle. However most of the other five rocks tested by Huck and Singh with the long duration jet have high values of specific energy (the dashed line in Fig. 19). This is due to wasted kinetic energy as the long duration jet erodes a deep hole and loses erosion capability by jet mixing which decreases the jet stagnation pressure. The length to diameter ratio of the slugs of water they used was at least 10^6 .

The much lower specific energies with the Voitsekhovskiy nozzle are believed to be due in part to the larger jet diameter which maintains pressure to greater depths in the eroded hole and therefore can initiate large shear fractures. Also the short length to diameter ratio (about 200) of the initial portion of the jet, which carries most of the kinetic energy, implies that the jet is terminated before the eroded hole is so deep that only ineffective further erosion can occur. The advantage in using values of length-to-diameter ratio less than 1000 has been previously pointed out. (Ref. 4).

In Fig. 19 are also shown two points with "specific energies" of 17 and 13 J/cm^3 which are based on the volume of large chunks which were split off from the 30 cm cubic granite samples. A similar value of 20 J/cm^3 is plotted for sandstone. These points of course are not relevant for predicting behavior of rock in situ or in larger samples. The values of "specific energy" observed for these cases of split off are greatly dependent on the particular size and geometry of the rock sample, as well as the jet direction relative to cleavage planes.

The three points for tests against granite with vacuum in the nozzle are also shown in Fig. 19. Two of these points (Shots 42 and 43) show quite high values of specific energy which do not appear to fall on the same curve as the data taken with air in the nozzle. The size of the craters was unexpectedly small at these high jet stagnation pressures. Further tests are needed with vacuum in the nozzle and with a standoff distance less than 15 cm to determine whether these points are anomalous. However the limestone point tends to confirm them.

8.0 CONCLUSIONS

For cratering of granite and sandstone using pulsed water jets from a Voitsekhovskiy-type nozzle with ambient air in the nozzle, the specific energy decreases very rapidly as the

pressure is raised from 1.43 to 3.95 times the compressive strength of the rock. Values of specific energy as low as 500 J/cm^3 were observed for Barre granite with a piston energy of 45,000 Joules and a measured jet velocity of only 1050 m/sec. (An estimated jet stagnation pressure of 560 MN/m^2). With jet velocities in the range from 925 to 1130 m/sec, "split off" fracture of large sections of the 30 cm cubic samples of granite was observed. Therefore, larger samples or in situ testing are required to provide data applicable for tunneling. In the tests with Indiana limestone, extensive splitting and shattering of the rock samples was observed with jet velocities from 1160 to 1450 m/sec. Berea sandstone was split with a jet velocity of only 420 m/sec.

No significant mechanical damage to the nozzle has been observed after a total of 43 test shots.

There was some evidence that the standoff distance from the nozzle to the rock should be quite short, about 7.5 to 15 cm, in order to achieve most effective rock breakage.

9.0 RECOMMENDATIONS

Additional tests with larger rock samples should be conducted with both air and vacuum in the Russian-made nozzle in order to extend the test data to higher jet stagnation pressures and other types of rock.

Tests should also be made with the American-made nozzle which has a larger area ratio (small exit diameter) and is designed for higher jet stagnation pressures.

REFERENCES

1. Voitsekhovskiy, B.V. et al, "Some Results of the Destruction of Rocks by Means of a Pulsed Water Jet", News of the Siberian Branch of the USSR Academy of Sciences, Series of Technical Sciences, No. 1 (2), Novosibirsk, pp. 7-11.
2. Clipp, L.L. & Cooley, W.C., "Development, Test and Evaluation of an Advanced Design Experimental Pneumatic Powered Water Cannon", Exotech, Inc. Final Technical Report TR-RD-040 for the U.S. Army Mobility Equipment Research and Development Center, Contract DAAK 12-68-C-0444, March 1969.
3. Huck, P.J. and Singh, M.M., "Rock Fracture by High Speed Water Jet", IIT Research Institute Final Report No. FRA-RT-71-58 for U.S. Dept. of Transportation, Federal Railroad Administration, December, 1970.
4. Cooley, W.C., "Correlation of Data on Erosion and Breakage of Rock by High Pressure Water Jets", Chapter 33 in "Dynamic Rock Mechanics", Edited by George B. Clark, American Institute of Mining, Metallurgical & Petroleum Engineers, New York, 1971
5. Voitsekhovskiy, B.V., "Jet Nozzle for Obtaining High Pulse Dynamic Pressure Heads", "U.S. Patent No. 3,343,794, Sept. 26, 1967.
6. Voitsekhovskiy, B.V., Personal communication to W.C. Cooley, June, 1971
7. Cooley, W.C., Beck, F.L. and Jaffe, D.L., "Design of a Water Cannon for Rock Tunneling Experiments", Terraspace, Inc. Final Report No. FRA-RT-71-70 for U.S. Dept. of Transportation Contract DOT-FR-00017, February 1971.

APPENDIX A

Design of the American-Made Nozzle

The design of the American-made nozzle (See Fig. A-1) was based on information obtained from Prof. B.V. Voitsekhovskiy by W.C. Cooley in a personal visit to Novosibirsk in 1970. The internal geometry of the exponential section was nearly identical to one of the nozzles which had been made in the U.S.S.R.

The structural design was based on stress analysis which had been conducted previously by Terraspace and by Pressure Science, Inc. for a larger nozzle which was designed for the U.S. Department of Transportation (Ref. 7). The interferences required on the tapered interfaces between the inner and outer sleeves of each nozzle section were reduced from those for the larger nozzle in proportion to the interface diameters.

The entrance chamber of the nozzle had a bore diameter of 8.35 cm (3.29 in.) in order to accept pistons of 3.25 in. diameter which were fired from the gas gun. The nominal design point of the nozzle requires a piston velocity of 220 m/sec (720 ft/sec) in order to start filling the nozzle with the same volume flow rate as achieved by Prof. Voitsekhovskiy in his tests.

The nozzle is designed for a maximum internal pressure of 200,000 psi, which should permit attainment of a maximum jet stagnation pressure of 800,000 psi with an exit diameter of 0.6 cm (0.236 in.)

Problems have been encountered in manufacture of Sections 2 and 4 of the nozzle. (Section 1 was successfully used with the Russian nozzle) During assembly, the outer sleeve of Section 2 failed in tension due to a flaw in the AISI 4340 steel which was used. A new part was made and successfully assembled. The outer sleeve of Section 4 failed several days after pressing together the two sleeves. This was believed to be caused by stress corrosion or hydrogen embrittlement. A new part was made, but it also failed approximately five minutes after assembly. Inspection is underway to identify the cause of this failure.

It is hoped that the nozzle can be completed by April 1, 1972.

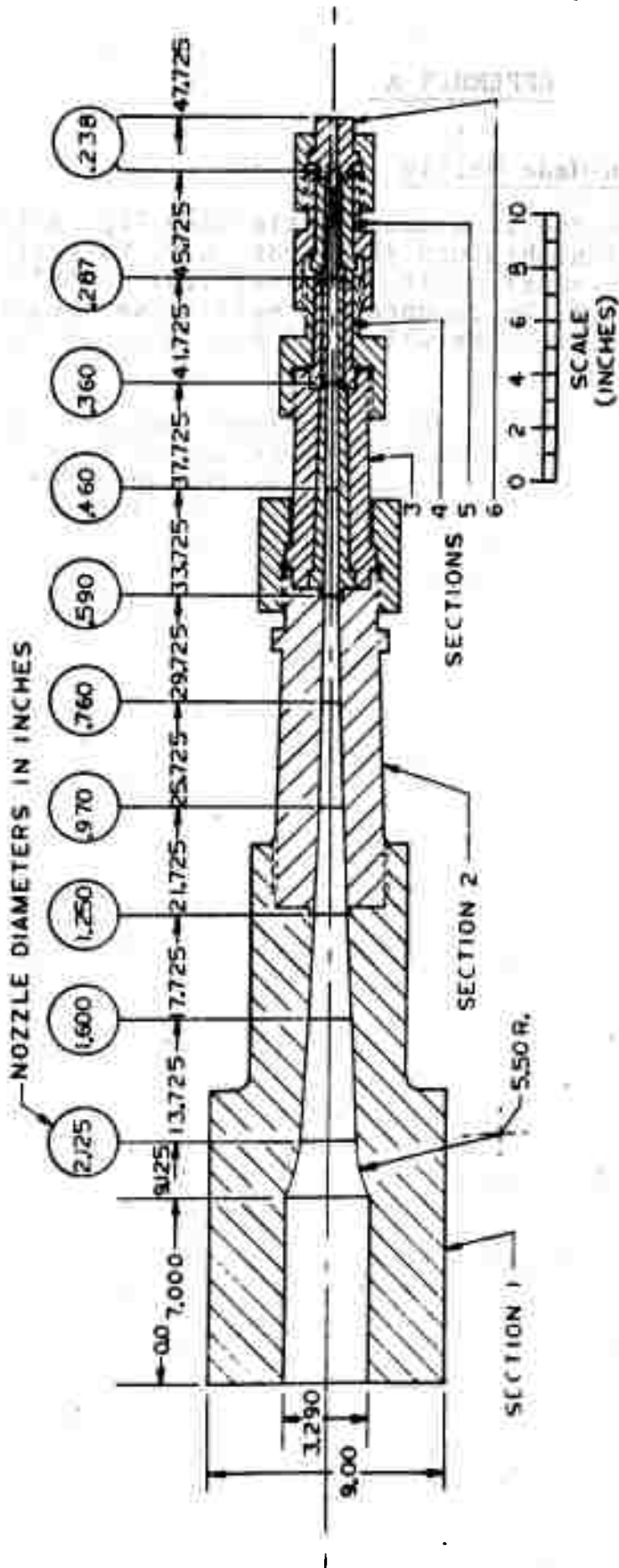


Fig. A-1 Drawing of American Design Nozzle